ELSEVIER

www.elsevier.nl/locate/jorganchem

Journal of Organometallic Chemistry 614–615 (2000) 113–119

Journal of Organometallic Chemistry

Rhodium cyclooctadiene complexes of the weakly co-ordinating carborane anion [*closo*-$CB_{11}H_{12}]^-$. Isolation and crystal structures of [(COD)Rh(η^2-$CB_{11}H_{12}$)] and [(COD)Rh$(THF)_2$][$CB_{11}H_{12}$]

Andrew S. Weller [a,*], Mary F. Mahon [a], Jonathan W. Steed [b]

[a] *Department of Chemistry, University of Bath, Bath, BA2 7AY, UK*
[b] *Department of Chemistry, Kings College London, The Strand, London, WC2R 2LS, UK*

Received 27 March 2000

Dedicated to Prof. Sheldon Shore, on the occasion of his 70th birthday, in recognition of the many outstanding contributions he has made to cluster science.

Abstract

Reaction of Ag[$CB_{11}H_{12}$] with [Rh(COD)Cl]$_2$ (COD = 1,4-cyclooctadiene) affords the complex [Rh(COD)(η^2-$CB_{11}H_{12}$)] (**2**), which has been characterised by NMR spectroscopy and X-ray crystallography. The solid-state structure shows that the carborane is co-ordinated to the rhodium by two 3c–2e Rh–H–B bonds. The solution fluxional behaviour of the {Rh(COD)} fragment over the surface of the cage is discussed. The carborane ligand in **2** is displaced by THF to give the crystallographically characterised complex [(COD)Rh$(THF)_2$][$CB_{11}H_{12}$] (**3**). Complex **3** is a structurally characterised model for the active species in [Rh$(L_2)(S)_2]^+$ (L = bidentate ligand, S = weakly bound solvent) Lewis-acid catalysed hydrogenation and hydroacylation reactions. It is suggested that the low nucleophility of [$CB_{11}H_{12}]^-$ is an important factor in the isolation of **3**.

Keywords: Weakly co-ordinating; Carborane; Rhodium

1. Introduction

The chemistry of icosahedral monocarborane anions, such as [1-*closo*-$CB_{11}H_{12}]^-$ (**1**), is an important and developing area, as their weakly co-ordinating properties are being increasingly appreciated in the stabilisation of highly Lewis-acidic species [1]. The combination of chemical robustness, delocalised negative charge, low nucleophilicity and potential for surface functionalisation have tagged these anions as the 'least co-ordinating' anions known to date [2]. This label has been justified by the isolation of protonated benzene as a stable crystalline salt [3], the characterisation of the closest approach to the long sought trialklysilylium ion [4] and the isolation and structural characterisation of $[Cu(CO)_4]^+$ [5], amongst others. Given the promise of monocarborane anions to act as partners with strongly Lewis-acidic centres, which find applications in many metal-mediated organic transformations, such as α-olefin polymerisation [6] and transition metal mediated enantio-selective catalysis [7], the chemistry of *closo* carborane anions, especially those derived from [1-*closo*-$CB_{11}H_{12}]^-$, with transition-metal centres is surprisingly underdeveloped. Complexes formed with Group 4 metallocenes have received some attention [8], while isolated examples of group **8** (Fe) [9], **9** (Ir) [10] and **10** (Pt) [11] transition metal complexes intimately linked with [1-*closo*-$CB_{11}H_{12}]^-$ have been reported. The solid-state structures of the silver salts for a range of carborane anions derived from **1** have also been investigated [12].

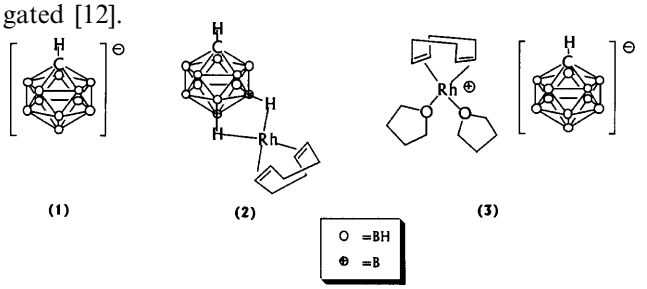

* Corresponding author.
E-mail address: a.s.weller@bath.ac.uk (A.S. Weller).

0022-328X/00/$ - see front matter
PII: S0022-328X(00)00608-2

We are embarking on a systematic investigation of the synthesis, structures and reactivity of the transition metal complexes of these least co-ordinating carborane anions. As part of this study, we report here the synthesis and characterisation – both solution and solid-state of a complex formed between [1-*closo*-$CB_{11}H_{12}]^-$ (**1**), and $\{Rh(COD)\}^+$ (COD = 1,4-cyclooctadiene). We also present the structural characterisation of a THF solvated species that acts as a structural model for the active species in rhodium based Lewis-acid catalysed hydrogenation reactions.

2. Results and discussion

2.1. Synthesis and structure of [Rh(COD)(η^2-$CB_{11}H_{12}$)]

Reaction of two equivalents of $Ag[CB_{11}H_{12}]$ with $[RhCl(COD)]_2$ in CH_2Cl_2 for 4 h affords [Rh(COD)(η^2-$CB_{11}H_{12}$)] (**2**) in good yield. Compound **2** was characterised by NMR spectroscopy and single crystal X-ray diffraction. The solid-state structure of **2** is shown in Fig. 1.

The rhodium co-ordination sphere in **2** is best described as being distorted square planar, bracketed by cyclooctadiene and carborane ligands. The {Rh(COD)} fragment is slightly canted from lying on the mirror planes partly-defined by B(7)–Rh(1)–B(12) and Rh(1)–X–Y by 11.1°, probably due to packing effects in the solid-state (X and Y = midpoint of the C=C bonds). The bond lengths and angles of the cyclooctadiene ligand are unremarkable, while the $Rh-C_{alkene}$ bonds lengths are as expected for a Rh(I) metal centre co-ordinated to an alkene [13], lying in the range 2.117(3)–2.129(3) Å. These distances are slightly shorter than those found in the *exo-nido* rhodaphosphacarborane [Rh(7-PPh_2-8-Me-7,8-*nido*-$C_2B_9H_{10}$)(COD)], viz. 2.104(4) and 2.106(4) Å for the $Rh-C_{alkene}$ bonds *trans* to BH [14]. The single carbon atom in the cage [C(1)] was unambiguously located. The carborane ligand is bound to the Rh(1) in an η^2 mode through two B–H–Rh 3 centre–2 electron bonds, using the antipodal BH group [H(12)] – as expected since this hydrogen is also bound to the most negatively charged boron atom- and one of the hydrogen atoms [H(7)] in the lower pentagonal belt. These μ-H atoms were located but not refined freely (see Section 3), so a detailed discussion of Rh–H bond lengths is not warranted. The Rh–B distances, at 2.391(3)Å [Rh(1)–B(7)] and 2.385(3) Å [Rh(1)–B(12)] are similar to those found in other *exo-nido* rhodacarboranes, such as [*exo-nido*-4,9-{$(PPh_3)_2Rh$}-4,9-μ-$(H)_2$-7-Me-8-Ph-7,8-$C_2B_9H_8$] [2.36(1) and 2.40(1) Å] [15]. Salient bonds lengths and angles for complex **2** can be found in Table 2. Crystallographically characterised examples of *exo*-B–H–Rh bonds in icosahedrally based systems are relatively rare, examples including the *exo-nido* complexes described by Hawthorne, such as [*exo-nido*-{$Rh(PPh_3)_2$}7-Me-8-Ph-7,8-$C_2B_9H_{10}$] [15], and Stone [10-*endo*-{$Au(PPh_3)$}-5,10-(μ-$H)_2$-*exo*-{$Rh(PPh_3)_2$}-7,8-Me_2-*nido*-$C_2B_9H_7$] [16], [$ReRh(CO)_3(\eta^5$-$C_5Me_5)(\eta^5$-7-$CB_{10}H_{11})$] [17]. The only previously reported example of η^2-co-ordination of a *closo* monocarborane is in [Pt{$R_2P(CH_2)_3PR_2$}(*closo*-$CB_{11}H_{12}$)][$CB_{11}H_{12}$] (R = Bu^t) [11], which displays a similar bi-dentate, co-ordination mode to that found in **2**.

The room temperature ^{1}H-NMR spectrum of complex **2** displays resonances attributable to the cyclooctadiene and carborane moieties. Only three peaks are observed for the COD ligand, at δ 4.96, 2.41 and 1.87 ppm, all equivalent to 4H, indicating that this ligand

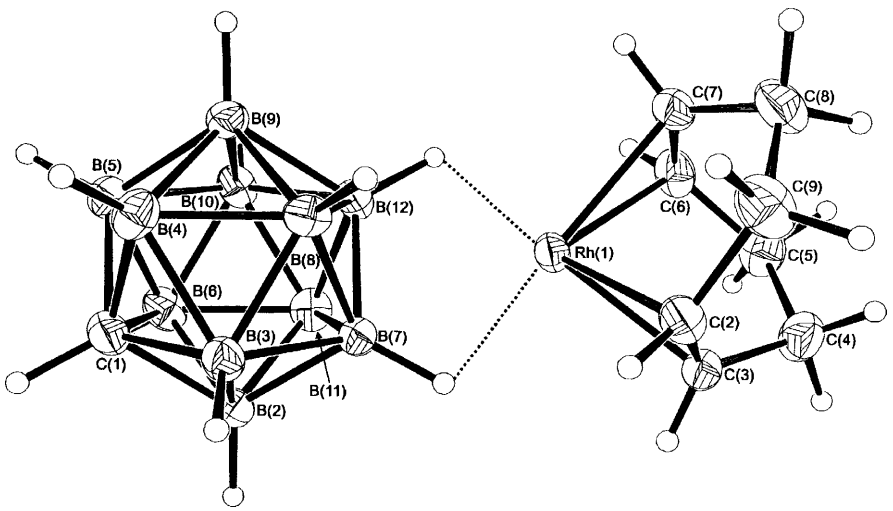

Fig. 1. ORTEX drawing of compound **2**, showing the compound numbering scheme. Hydrogen atoms are shown with an arbitrary radius, while thermal ellipsoids are drawn at the 30% probability level.

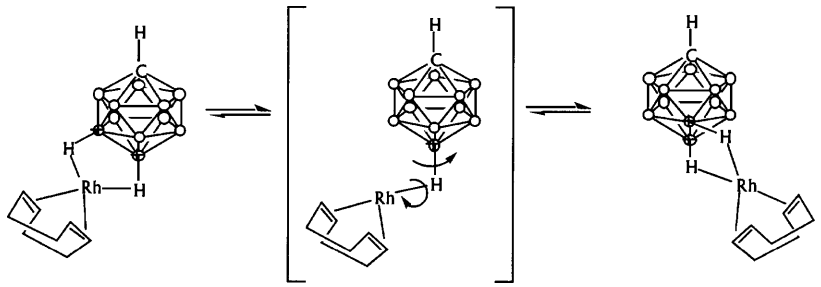

Scheme 1. Proposed fluxional mechanism operating in compound **2**.

experiences a symmetrical time-averaged environment at room temperature. A broad, integral 1H, singlet at δ 2.61 ppm is assigned to the cage C–H group, while the BH protons are observed as three peaks in the $^1H\{^{11}B\}$-NMR spectrum, in the ratio 5:5:1, at δ 1.86, 0.06 and -3.92 ppm, respectively. The latter two peaks are shifted by ca. δ 1.8 and 5.0 ppm upfield, respectively, compared with **1**. The highest field, integral one peak, which is assigned to the antipodal bridging hydrogen atom, H(12), is observed in the ^1H-NMR spectrum as a quartet, J(BH) 109 Hz. The reduction in the value of the BH coupling constant, compared with terminal BH (ca. 140–150 Hz), is as expected for co-ordination to a metal centre, consistent with weakening of the B–H bond. The expected Rh–H coupling is not observed for this peak under any of the conditions investigated and is presumably small (peak width at half height at 298 K in the $^1H\{^{11}B\}$ spectrum is ca. 15 Hz). Similar behaviour has been observed previously in analogous *exo-nido* Rh systems [18]. The peak at δ 0.06 ppm is assigned to the five B*H* atoms in the lower pentagonal belt of the carborane cage, which are equivalent at room temperature, which contrasts with the asymmetric solid-state structure, indicating that a fluxional process is occurring (vide infra). In the ^1H-NMR spectrum this peak is observed as a broad quartet, J(BH) 130 Hz. The room temperature $^{11}B\{^1H\}$-NMR spectrum (128 MHz) shows two peaks at δ -15.5 ppm and -16.2 ppm, of relative intensity 5B and 6B respectively, which both split into doublets on coupling to ^1H. The small chemical shift difference ($\Delta\delta_{11B} = 0.7$ ppm) between these two peaks made $^1H\{^{11}B$-selective$\}$ decoupling experiments ambiguous. However, on the basis of the chemical shift changes from free $[CB_{11}H_{12}]^-$ we assign the lower field peak to the boron atoms in the lower pentagonal belt, as this peak has moved significantly upfield ($\Delta\delta_{11B}$ ca. 2 ppm from the free anion) [19] – consistent with co-ordination to a metal centre. We were unable to observe the peak due to the unique boron atom [B(12)], but on the basis of relative intensities it is masked by the peak at δ -16.2 ppm. Making this assumption, the unique boron shifts at least 8 ppm to high field on co-ordination to the metal fragment. The observation of such a simple ^{11}B-NMR spectrum, is further confirmation that the molecule is fluxional at room temperature.

Cooling a sample of **2** to -90°C (CD_2Cl_2 solution) did not result in any appreciable change in peak positions in the ^1H- and $^1H\{^{11}B\}$-NMR spectra, indicating that any fluxional process occurring is very facile. The peak at δ -3.92 ppm does broaden significantly at lower temperatures in the $^1H\{^{11}B\}$-NMR spectrum, perhaps indicative of some residual Rh–H coupling, as at lower temperatures thermal decoupling of boron is expected to sharpen peaks [20]. A plausible mechanism to account for the observed NMR spectra is one in which the {Rh(COD)} fragment stays bound to H(12) and processes around the lower pentagonal belt of the carborane, thus rendering the five associated hydrogen atoms equivalent (Scheme 1). This process alone would not afford equivalence of the diene protons – contrary to observation – so an additional, facile, rotation of the COD ligand around the Rh centre must also be occurring (scheme). Related mechanisms have been postulated previously for $\{Pt(L\text{-}L)\}^+$ [(L-L) – bidentate phosphine] fragments bound to $[CB_{11}H_{12}]^-$ [11] and $\{RhL_2\}^+$ (L = phosphine) fragments bound *exo-nido* to [7,8-*nido*-$C_2B_9H_{12}]^-$ and its derivatives [15,21].

2.2. Reaction of complex **2** with THF

$[Rh(L_2)(solvent)_2]^+$ (L = bidentate phosphine, weakly bound solvent = THF, CH_2Cl_2) are important reagents in Lewis acid catalysed hydrogenation [7] and hydroacylation [22] reactions. Given their widespread use in organic chemistry it is surprising that these complexes, to our knowledge, have not been structurally characterised. This is probably due, in part, to the counterions commonly paired with these reactive species, such as $[BF_4]^-$, which result in species that are either difficult to characterise or unamenable to crystallisation. The low nucleophility of the carborane anion $[CB_{11}H_{12}]^-$ prompted us to investigate the synthesis and structure of the THF solvated complex of **2**, which would be expected to be a direct analogue of $[Rh(L_2)(solvent)_2]^+$.

Dissolution of **2** in THF immediately resulted in a colour change from orange to yellow. The $^{11}B\{^1H\}$-NMR spectrum showed that only free $[CB_{11}H_{12}]^-$ was

present in solution, demonstrating that THF had displaced the carborane cage from the co-ordination sphere of rhodium, forming $[Rh(COD)(THF)_2][CB_{11}H_{12}]$ (**3**). Crystals grown from layering a THF solution of **3** with hexanes were extremely susceptible to solvent loss (THF), but a suitable crystal, quickly cooled to 100 K on removal from the mother liquor, afforded a satisfactory X-ray structural determination. Unfortunately, due to solvent loss in the lattice combined with a badly twinned crystal, the refined structure only yields the gross structural features ($R_1 = 0.0884$), further compounded by the difficulty in locating the cage C atom. Nevertheless, it can be clearly seen (Fig. 2, Table 3) that the rhodium is square planar co-ordinated [difference in the dihedral angle between the two planes (vide supra) being 1.8°, greatest deviation from the square-plane defined by Rh(1)–O(1)–O(2)–X–Y is 0.018 Å (where X and Y are the mid-points of the C=C bonds)], with two THF molecules complementing the cyclooctadiene ligand around the Rh centre, Rh(1)–O(1) 2.154(5) Å, Rh(1)–O(2) 2.135(6) Å. The carborane cage is not bound to the metal, the closest BH···Rh distance being ca. 3.0 Å for H(12)···Rh(1). Crystallographically characterised THF solvated Rh complexes are rare [23], while complex **3** is the first mononuclear complex of this type characterised by X-ray crystallography. Dissolution of crystalline **3** in CD_2Cl_2 immediately (< 5 min) generated complex **2** and free THF (by ^{1}H-NMR spectroscopy).

Recent reports of the oligomerization of 3,3-dimethylbutyne promoted by $[Rh(COD)(solvent)_2][BF_4]$ [24] – that shows changes in product distribution on changing the co-ordinated solvent (THF and MeCN) – along with the strong anion dependence observed in the mechanism of enantioselective hydrogenation reactions by $[Rh(P_2)(solvent)]^+$ complexes [25] (P_2 = bidentate phosphine), suggests that complex **2** may show different reactivity patterns to those previously observed due to the presence of the weakly ligated carborane anion in the co-ordination sphere. We are currently investigating this possibility in **2** and related compounds in a number of transition metal catalysed reactions and intend to report on this at a later date.

3. Experimental

3.1. General methods

All manipulations were carried out under an argon atmosphere using standard Schlenk line or drybox techniques. CH_2Cl_2 was distilled from CaH_2, hexane was distilled from sodium [26]. The starting materials $Ag[CB_{11}H_{12}]$ (**1**) [12c] and $[Rh(COD)Cl]_2$ [27] were prepared by the literature routes. NMR spectra were measured on a Varian-400 or JEOL-270 FT-NMR spectrometer in CD_2Cl_2 solutions. Residual protio solvent was used as reference (δ, ppm: CD_2Cl_2 5.25) in ^{1}H-NMR, while $BF_3{\cdot}OEt_2$ (external) was used as refer-

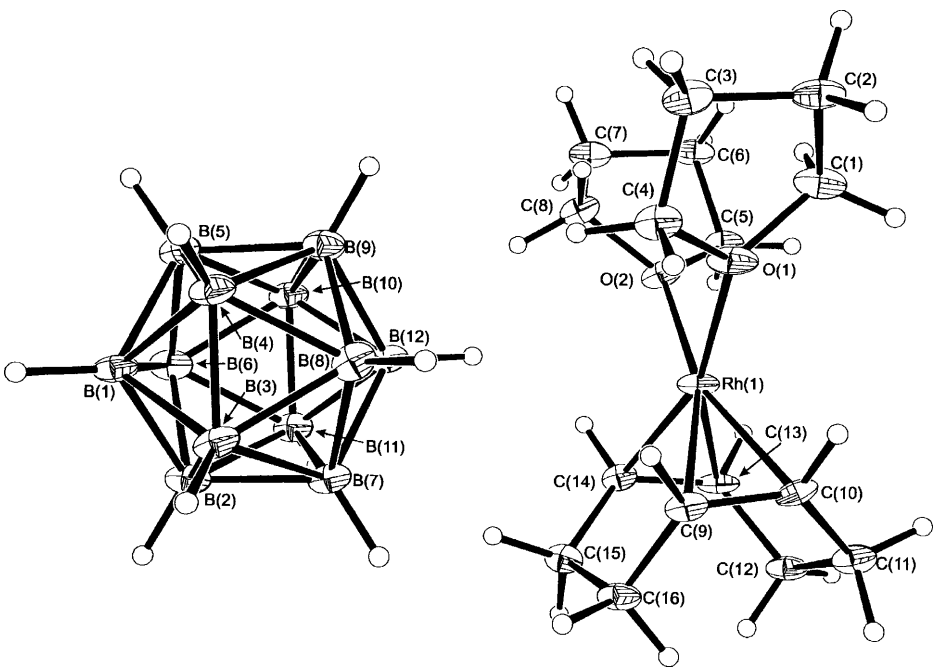

Fig. 2. ORTEX drawing of compound **3**, showing the compound numbering scheme. Hydrogen atoms are shown with an arbitrary radius, while thermal ellipsoids are drawn at the 30% probability level. The cage carbon atom was not located (see Section 3).

Table 1
Crystallographic data for the new complexes **2** and **3**

	2	**3**
Empirical formula	$C_9H_{24}B_{11}Rh$	$C_{17}H_{40}B_{11}O_2Rh$
Formula weight	354.10	498.31
Temperature (K)	293(2)	100(2)
Wavelength (Å)	0.71069	0.71073
Crystal system	Monoclinic	Triclinic
Space group	$P2_1/c$	$P\bar{1}$
Unit cell dimensions		
a (Å)	6.8910(10)	10.418(6)
b (Å)	17.826(2)	10.595(5)
c (Å)	13.0560(10)	11.443(8)
α (°)	90	97.14(4)
β (°)	96.280(10)	95.66(3)
γ (°)	90	99.72(4)
Volume (Å^3)	1594.2(3)	1225.9(13)
Z	4	2
D_{calc} (Mg m^{-3})	1.475	1.350
Absorption coefficient (mm^{-1})	1.049	0.709
F(000)	712	516
Crystal size (mm)	$0.20\times0.20\times0.18$	$0.20\times0.20\times0.15$
θ Range for data collection (°)	2.28–24.97	2.00–25.00
Reflections collected	3146	8076
Independent reflections	2791 [$R_{int}=0.0190$]	4287 [$R_{int}=0.0541$]
Refinement method	Full-matrix least-squares on F^2	Full-matrix least-squares on F^2
Data/restraints/parameters	2791/0/219	4287/0/280
Goodness-of-fit on F^2	0.607	1.126
Final R indices [$I>2\sigma(I)$]	$R_1=0.0237$, $wR_2=0.0695$	$R_1=0.0884$, $wR_2=0.1884$
R indices (all data)	$R_1=0.0328$, $wR_2=0.0758$	$R_1=0.0953$, $wR_2=0.1915$
Largest difference peak and hole (e Å^{-3})	0.352 and −0.261	6.239 and −1.542

ence in ^{11}B-NMR spectra. Coupling constants are given in Hz. Infrared spectra were measured on a Perkin–Elmer 1600 FT spectrometer. Elemental analysis was performed in-house in the Department of Chemistry, University of Bath.

3.2. X-ray crystallography

For complex **2**, crystallographic measurements were made on a CAD4 automatic four-circle diffractometer. Crystals of complex **3** were mounted on a thin glass fibre using silicon grease and cooled on the diffractometer (Nonius ^{Kappa}CCD) to 100 K using an Oxford Cryostream low temperature attachment. Data were corrected for Lorentz and polarisation and also for extinction and crystal decay. Both structures were solved using SHELXS-97 [28] and developed via alternating least-squares cycles and difference Fourier synthesis (SHELXL-97). In the final least-squares cycles all atoms were allowed to vibrate anisotropically, while hydrogen atoms are assigned an isotropic thermal parameter 1.2 times that of the parent atom (1.5 for terminal atoms) and allowed to ride. It was possible to positionally refine the protons attached to B(7) and B(12) in complex **2**, however as 'free' refinement yielded final positions which were close (within the bounds of experimental error) to the calculated positions, these hydrogens were ultimately refined riding on the parent atoms. The asymmetric units (shown in Figs. 1 and 2), along with the labelling scheme used was produced using ORTEX [29]. Due to solvent loss in the crystal coupled with a gross twinning problem, the residual R factor for complex **3** was found to be poor and the cage carbon atom was not located. Crystallographic data and selected bond distances and angles are given in Tables 1–3, respectively.

3.3. [Rh(cod)][η^2-$CB_{11}H_{12}$] (2)

[Rh(cod)Cl]$_2$ (0.138 g, 0.56 mmol) and Ag[$CB_{11}H_{12}$] (0.140 g, 0.56 mmol) were stirred in CH_2Cl_2 (20 cm^3) for 16 h. The solution was filtered through a Celite pad to remove AgCl, and the solvent removed in vacuo to minimum volume. Hexanes (20 cm^3) were added to precipitate the product as an orange powder. Recrystallisation from CH_2Cl_2–hexane afforded orange crystals of [Rh(cod)][η^2-$CB_{11}H_{12}$] (0.180 g, 91%). Calc.: H, 6.79; C, 30.5. Found: H, 6.39; C, 29.9%.

3.3.1. NMR data

^{1}H: 4.96 (m, 4H, C_{alkene}–*H*), 2.61 (s br, 1H, C_{cage}–*H*), 2.41 (m, 4H, C*H*$_2$), 1.87 (m, 4H, C*H*$_2$), 1.86 (br pcq, 5H, B*H*), 0.06 [br pcq, *J*(BH) 130, 5H, B*H*], −3.92 (pcq, 1H, *J*(BH) 109, B*H*). Selected ^{1}H{^{11}B}: 1.86 (5H, B*H*), 0.06 (5H, B*H*), −3.92 (1H, B*H*). ^{11}B{^{1}H}: −15.5 (ca. 5B), −16.2 (ca. 6B).

3.4. [Rh(cod)(THF)$_2$][$CB_{11}H_{12}$] (3)

[Rh(cod)][η^2-$CB_{11}H_{12}$] (0.030 g, 0.085 mmol) was dissolved in THF (1 cm^3), with a concomitant colour change from orange to yellow. Conversion was quantitative by ^{1}H- and ^{11}B-NMR spectroscopy. Recrystallisation by solvent diffusion into hexanes afforded X-ray quality crystals of [Rh(cod)(THF)$_2$][$CB_{11}H_{12}$], which lost solvent (THF) rapidly on removal from the mother liquor. Dissolution of the crystals in CD_2Cl_2 regenerated **2** in quantitative yield. Due to solvent loss a reasonable microanalysis was not obtained.

3.4.1. NMR data

^{11}B{^{1}H} (H_8–THF): −7.7 (1B), −13.6 (5B), −15.8 (5B).

Table 2
Selected bond lengths (Å) and angles (°) for **2**

Rh(1)–C(6)	2.117(3)	Rh(1)–C(2)	2.120(3)
Rh(1)–C(7)	2.127(3)	Rh(1)–C(3)	2.129(3)
Rh(1)–B(12)	2.385(3)	Rh(1)–B(7)	2.391(3)
B(2)–C(1)	1.708(5)	B(2)–B(7)	1.758(5)
B(2)–B(6)	1.777(5)	B(2)–B(11)	1.787(5)
B(2)–B(3)	1.791(5)	B(3)–C(1)	1.705(4)
B(3)–B(7)	1.764(4)	B(3)–B(8)	1.770(5)
B(3)–B(4)	1.786(5)	B(4)–C(1)	1.719(5)
B(4)–B(8)	1.755(5)	B(4)–B(5)	1.762(5)
B(4)–B(9)	1.773(5)	B(5)–C(1)	1.705(4)
B(5)–B(9)	1.744(5)	B(5)–B(10)	1.756(5)
B(5)–B(6)	1.756(5)	B(6)–C(1)	1.708(5)
B(6)–B(11)	1.759(5)	B(6)–B(10)	1.779(5)
B(7)–B(12)	1.744(4)	B(7)–B(11)	1.782(5)
B(7)–B(8)	1.783(5)	B(8)–B(12)	1.781(4)
B(8)–B(9)	1.789(4)	B(9)–B(12)	1.767(5)
B(9)–B(10)	1.790(5)	B(10)–B(12)	1.764(4)
B(10)–B(11)	1.797(5)	B(11)–B(12)	1.780(5)
C(2)–C(3)	1.384(5)	C(2)–C(9)	1.516(5)
C(3)–C(4)	1.506(4)	C(4)–C(5)	1.508(5)
C(5)–C(6)	1.499(5)	C(6)–C(7)	1.381(5)
C(7)–C(8)	1.508(5)	C(8)–C(9)	1.503(5)
C(6)–Rh(1)–C(2)	97.23(13)	C(6)–Rh(1)–C(7)	37.97(14)
C(2)–Rh(1)–C(7)	81.94(12)	C(6)–Rh(1)–C(3)	81.20(13)
C(2)–Rh(1)–C(3)	38.01(12)	C(7)–Rh(1)–C(3)	90.02(13)
C(6)–Rh(1)–B(12)	117.03(12)	C(2)–Rh(1)–B(12)	141.20(12)
C(7)–Rh(1)–B(12)	113.54(12)	C(3)–Rh(1)–B(12)	156.44(12)
C(6)–Rh(1)–B(7)	152.46(12)	C(2)–Rh(1)–B(7)	108.96(11)
C(7)–Rh(1)–B(7)	152.32(12)	C(3)–Rh(1)–B(7)	114.46(11)
B(12)–Rh(1)–B(7)	42.84(11)	B(12)–B(7)–Rh(1)	68.42(15)
B(2)–B(7)–Rh(1)	159.2(2)	B(3)–B(7)–Rh(1)	139.7(2)
B(11)–B(7)–Rh(1)	102.90(18)	B(8)–B(7)–Rh(1)	87.61(17)
B(7)–B(12)–Rh(1)	68.74(15)	B(10)–B(12)–Rh(1)	159.0(2)
B(9)–B(12)–Rh(1)	140.1(2)	B(11)–B(12)–Rh(1)	103.16(19)
B(8)–B(12)–Rh(1)	87.82(16)		

Table 3
Selected bond lengths (Å) and angles (°) for **3**

Rh(1)–C(14)	2.088(8)	Rh(1)–C(10)	2.097(8)
Rh(1)–C(9)	2.104(7)	Rh(1)–C(13)	2.111(7)
Rh(1)–O(2)	2.135(6)	Rh(1)–O(1)	2.154(5)
C(14)–Rh(1)–O(2)	89.8(3)	C(10)–Rh(1)–O(2)	159.2(3)
C(9)–Rh(1)–O(2)	162.4(3)	C(13)–Rh(1)–O(2)	93.9(3)
C(14)–Rh(1)–O(1)	160.0(3)	C(10)–Rh(1)–O(1)	90.3(3)
C(9)–Rh(1)–O(1)	94.3(3)	C(13)–Rh(1)–O(1)	161.2(3)
O(2)–Rh(1)–O(1)	86.4(2)		

4. Supplementary material

Tables of atomic co-ordinates and anisotropic temperature factors are available as supplementary data. Crystallographic data for the structures reported in this paper have been deposited with the Cambridge Crystallographic Data Centre, CCDC no. 141776 for compound **2** and CCDC no. 141777 for compound **3**. Copies of this information may be obtained free of charge from the Director, CCDC, 12 Union Road, Cambridge, CB2 1EZ, UK (fax: +44-1223-336-033; e-mail: deposit@ccdc.cam.ac.uk or http://www.ccdc.cam.ac.uk).

Acknowledgements

We thank the EPSRC and King's College London for the provision of the X-ray diffractometer and the Nuffield Foundation for the provision of computing equipment (J.W.S.). The Royal Society (A.S.W.) is thanked for financial support as are Johnson Matthey for the generous loan of platinum metal salts.

References

[1] C.A. Reed, Acc. Chem. Res. 31 (1998) 133.
[2] K. Shelly, C.A. Reed, Y.J. Lee, W.R. Scheidt, J. Am. Chem. Soc. 108 (1986) 3117.
[3] C.A. Reed, N.L.P. Fackler, K.-C. Kim, D. Stasko, D.R. Evans, P.D.W. Boyd, C.E.F. Rickard, J. Am. Chem. Soc. 121 (1999) 6314.
[4] Z. Xie, J. Manning, R.W. Reed, R. Mathur, P.D.W. Boyd, A. Benesi, C.A. Reed, J. Am. Chem. Soc. 118 (1996) 2922.
[5] S.M. Ivanova, S.V. Ivanov, S.M. Miller, O.P. Anderson, K.A. Solntsev, S.H. Strauss, Inorg. Chem. 38 (1999) 3756.
[6] B. Cornils, W.A. Herrmann (Eds.), Applied Homogeneous Catalysis with Organometallic Compounds, Wiley-VCH, 2000
[7] OjimaI. (Ed.), Catalytic Asymmetric Synthesis, Wiley-VCH, 1993
[8] D.J. Crowther, S.L. Borkowsky, D. Swenson, T.Y. Meyer, R.F. Jordan, Organometallics 12 (1993) 2897.
[9] D.J. Liston, Y.J. Lee, W.R. Scheidt, C.A. Reed, J. Am. Chem. Soc. 111 (1989) 6643 and references therein.
[10] D.J. Liston, C.A. Reed, C.W. Eigenbrot, W.R. Scheidt, Inorg. Chem. 26 (1987) 2739.
[11] G.S. Mhinzi, S.A. Litster, A.D. Redhouse, J.L. Spencer, J. Chem. Soc. Dalton Trans. (1991) 2769.
[12] (a) Z. Xie, C.-W. Tsang, E.T.-P. Sze, Q. Yang, D.T.W. Chan, T.C.W. Mak, Inorg. Chem. 37 (1998) 6444. (b) Z. Xie, C.-W. Tsang, F. Xue, T.C.W. Mak, J. Organomet. Chem. 577 (1999) 197. (c) K. Shelly, D.C. Finster, Y.J. Lee, W.R. Scheidt, C.A. Reed, J. Am. Chem. Soc. 107 (1985) 5995.
[13] A.G. Orpen, L. Brammer, F.H. Allen, O. Kennard, D.G. Waston, R. Taylor, J. Chem. Soc. Dalton Trans. (1989) S1.
[14] C. Viñas, R. Núñez, F. Teixidor, R. Kivekäs, R. Sillanpää, Organometallics 17 (1998) 2376.
[15] C.B. Knobler, T.B. Marder, E.A. Misuzawa, R.G. Teller, J.A. Long, P.E. Behnken, M.F. Hawthorne, J. Am. Chem. Soc. 106 (1984) 2990.
[16] J.C. Jeffery, P.A. Jelliss, F.G.A. Stone, J. Chem. Soc. Dalton Trans. (1993) 1073.
[17] J.C. Jeffery, P.A. Jelliss, L.H. Rees, F.G.A. Stone, Organometallics 17 (1998) 2258.
[18] J.A. Long, T.B. Marder, P.E. Behnken, M.F. Hawthorne, J. Am. Chem. Soc. 106 (1984) 2979.
[19] T. Jelinek, J. Plesek, S. Hermanek, B. Stibr, Collect. Czech. Chem. Commun. 51 (1986) 819.
[20] H. Beall, C.H. Bushweller, Chem. Rev. 73 (1973) 465.
[21] D.D. Ellis, P.A. Jelliss, F.G.A. Stone, Organometallics 18 (1999) 4982.

[22] R.W. Barnhart, D.A. McMorran, B. Bosnich, Chem. Commun. (1997) 589.
[23] P.A. Agaskar, F.A. Cotton, L.R. Falvello, S. Han, J. Am. Chem. Soc. 108 (1986) 1214.
[24] A.D. Burrows, M. Green, J.C. Jeffery, J.M. Lynam, M.F. Mahon, Angew. Chem. Int. Ed. Engl. 38 (1999) 3043.
[25] J.M. Buriak, J.C. Klein, D.G. Herrington, J.A. Osborn, Chem. Eur. J. 6 (2000) 139.
[26] D.F. Shriver, M.A. Drezdon, The Manipulation of Air-Sensitive Compounds, 2nd ed., Wiley-Interscience, New York, 1986.
[27] G. Giordano, R.H. Crabtree, Inorg. Synth. 28 (1990) 88.
[28] G.M. Sheldrick, SHELXL, A Computer Program for Crystal Structure Refinement, University of Göttingen, Germany, 1997.
[29] P. McArdle, J. Appl. Crystallogr. 28 (1995) 65.